Mine Water and the Environment (2023) 42:546–559
https://doi.org/10.1007/s10230-023-00953-3

TECHNICAL ARTICLE

Study of Roof Water Inrush Control Technology and Water Resources Utilization During Coal Mining in a Karst Area

Wenqiang Wang[1] · Zhenhua Li[1,2,3] · Feng Du[1] · Zhengzheng Cao[1] · Guosheng Li[1]

Received: 29 December 2022 / Accepted: 28 August 2023 / Published online: 13 November 2023

Abstract

Roof water inrush at the mine face and shortages of water resources are both problems in the karst mining area in southwestern China. In this study, field measurements, similar simulations, and theoretical analysis were conducted, a physical model of upward and downward mining in a test mine was constructed, and the dynamic evolution of water inrush and the mechanism of water inrush in karst roofs under different mining sequences were analysed. As a result, the problem of water inrush at the mine face was solved, and a method to utilize the karst groundwater water resources was proposed. The research showed that after downward mining, the maximum development height of the water-conducting fracture in coal seam 4 was 43.1 m, and the fracture mining ratio was 14.4. A water-inrush pathway formed at the connection between the mining-induced fractures and the roof karst aquifers, and the safe mining of coal seams 4 and 9 were threatened by water inrush from the goaf. So, the feasibility of upward mining was determined by the ratio test and "three zones" discrimination methods, and the evolution of water-inrush pathways during upward and downward-inclined mining were compared. Upward-inclined mining was proposed to control roof water inrush. Moreover, the quality of the water flowing into the goaf was compared with the Chinese standards for water use, and the water in the goaf of the lower coal group was suitable for water resource utilization. This research provides a basis for preventing and controlling roof water inrush disasters and for appropriate utilization of water resources in these mining areas.

Keywords Karst area · Roof water inrush · Water inrush pathway · Upward mining · Water resources utilization

Introduction

The geological conditions of coal occurrence in China are extremely complex. Due to distinctly different mining conditions, mine water hazards vary, especially in western and southwestern China (Dong et al. 2021; Zhang et al. 2022). In western China, coal mines are mainly threatened by sandstone aquifers above the coal seams (Ju et al. 2018; Li et al. 2022a, b, c), while those in southwestern China are mainly threatened by karst aquifers (Jiang et al. 2020a, b). Compared with the sandstone roof aquifers in western China, the problem of karst roof water in southwestern China is complicated, uncertain, and difficult (Jiang et al. 2020a, b), which brings great problems and challenges to safe and efficient recovery of the mining face (Li et al. 2022a, b, c). At the same time, coal mining in the karst mine area in southwestern China also wastes a great deal of karst water, which aggravates groundwater loss in the karst area (Suo et al. 2022).

Studies on evolution, prevention, and controlling water-conducting fractures in roof strata during coal mining have been widely reported (Chen et al. 2022a, b; Long et al. 2022; Qiu et al. 2022; Sun et al. 2021; Xu et al. 2022). Considering the distribution characteristics of the "three horizontal zones and three vertical zones" of mining-induced fractures in roof (Cheng et al. 2020; Li et al. 2022a, b, c), the

✉ Zhenhua Li
jzlizhenh@163.com

✉ Feng Du
fdu_cumt@126.com

[1] School of Energy Science and Engineering, Henan Polytechnic University, Jiaozuo 454003, Henan, China

[2] Collaborative Innovation Center of Coal Work Safety and Clean High Efficiency Utilization, Jiaozuo 454003, Henan, China

[3] Henan Mine Water Disaster Prevention and Control and Water Resources Utilization Engineering Technology Research Center, Henan Polytechnic University, Jiaozuo 454003, Henan, China

development height of different water-conducting fractures can be obtained under various mining geological and hydrogeological conditions using a variety of methods, including the double-end water-plugging leak detection (Zhang et al. 2019), borehole observation (Chen and Zhu 2020), drilling fluid consumption (Feng et al. 2021), microseismic monitoring (Xiao et al. 2020), transient electromagnetic (Yao et al. 2019), and micro-resistivity scanning methods (Liu et al. 2018). Also, comprehensive similar simulation and numerical simulation methods (Li et al. 2022a, b, c; Zha et al. 2020; Zhao et al. 2021) can be used to reveal the complete development of roof water conduction cracks. Although grout plugging, perforated suction, and drainage have been proposed to prevent and control roof water hazards (Gui et al. 2018; Ji et al. 2021; Wen et al. 2022; Zhu et al. 2022a, b), these methods are not suitable for the treatment of roof water inrush under a karst roof. Indeed, much less research has been conducted on the development of water-conducting fractures in karst conditions.

With respect to utilization of water resources in mines, abandoned mines are mainly used to establish underground water reservoirs (Chen et al. 2022a, b; Song et al. 2020; Zhang et al. 2021), to store atmospheric rainfall for industrial and agricultural water (Dong et al. 2019), to store energy and generate electricity (Zhang et al. 2020), or to utilize mine geothermal resources (Kumari and Ranjith 2019; Menendez et al. 2020; Zhu et al. 2022a, b). In contrast, research on the using water resources in operating mines is sparse.

Based on the hydrogeological conditions of the Xintian coal mine and changes in mine water inflow, physically similar simulations and field measurements were employed to investigate the evolution of water-conducting fractures in roof strata during current downward mining, and the feasibility of upward mining was established by theoretical analysis and physical simulation. A method to prevent and control karst roof water inrush was developed, along with a way to recycle mine water resources, improving mine safety and production efficiency.

Engineering Background

Hydrogeological Conditions of the Mining Area

The Xintian Coal Mine is located in of Qianxi County, Guizhou Province, China. This area has a typical karst landform, so most of the atmospheric precipitation flows underground. The primary fractures and karst caves of the area are relatively well developed, with the karst development decreasing with increased depth. There are a large number of karst fractures and beaded karst caves with connectivity in the limestone of the Yulongshan Member of the Yelang Formation. The upper submember is a strong aquifer, while the lower submember is a weak aquifer. The drilling data show that irregular fractures are developed in this area, the rock core is relatively broken and moderately complete; the maximum width of the fractures is about 3.0 cm, and there are small karst cavities with a diameter of 0.5–2.0 cm in some parts, indicating strong groundwater activity. The Changxing Formation is weakly fractured, making it a weak aquifer. Figure 1 shows the comprehensive histogram of the rock strata.

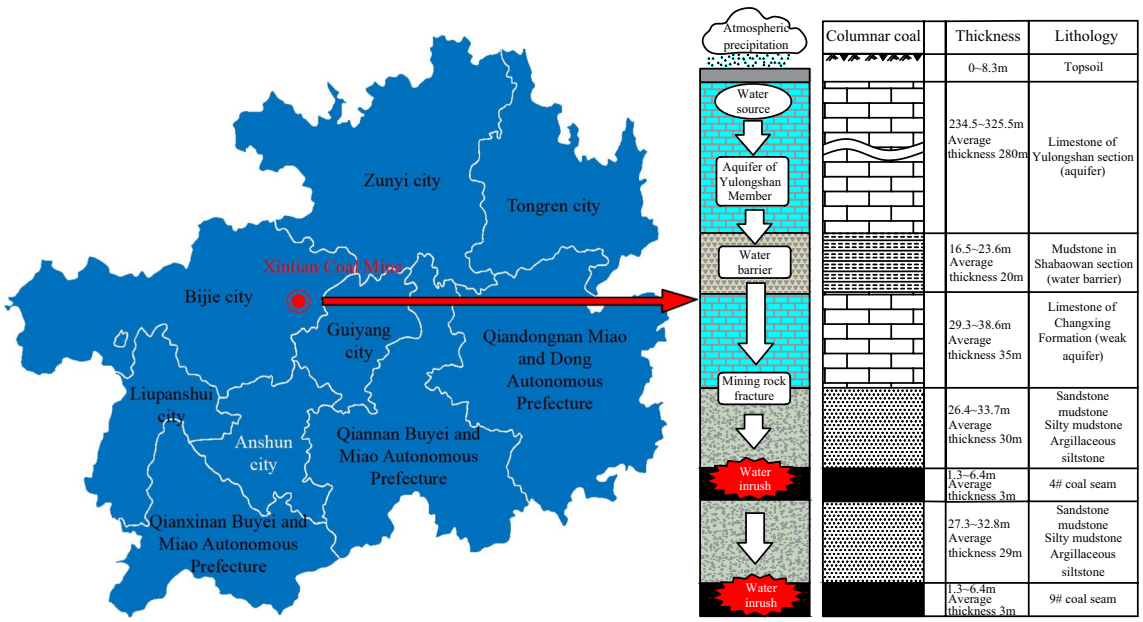

Fig. 1 Location of the study area and comprehensive Histogram of Rock Strata

Geological Conditions of the Mine

In the Xintian Coal Mine, coal seams 4 and 9 are the main seams being mined. The two seams have an average thickness of 3.0 m, with an average dip angle of 3°. The roof of coal seam 4 is 30 m and 85 m from the bottom interface of the Changxing Formation and Yulongshan Member limestone strata, while the roof of coal seam 9 is 62 m and 117 m respectively from the bottom interface of the Changxing Formation limestone and Yulongshan Member limestone. Based on the existing layout of the mine roadway and contour lines of the coal seam floor, inclined mining was the only choice. Currently, the upper part of coal seam 4 has been mainly exploited, as shown in Supplemental Fig. 1.

Analysis of Annual Water Inflow Change of Test Mine

Supplemental Fig. 2 shows the average monthly rainfall data at the mine site from 2017 to 2020. The mine water inflow was positively related to the atmospheric rainfall, especially during June to October. During this period, roof karst water entering the goaf through mining-induced water-conducting

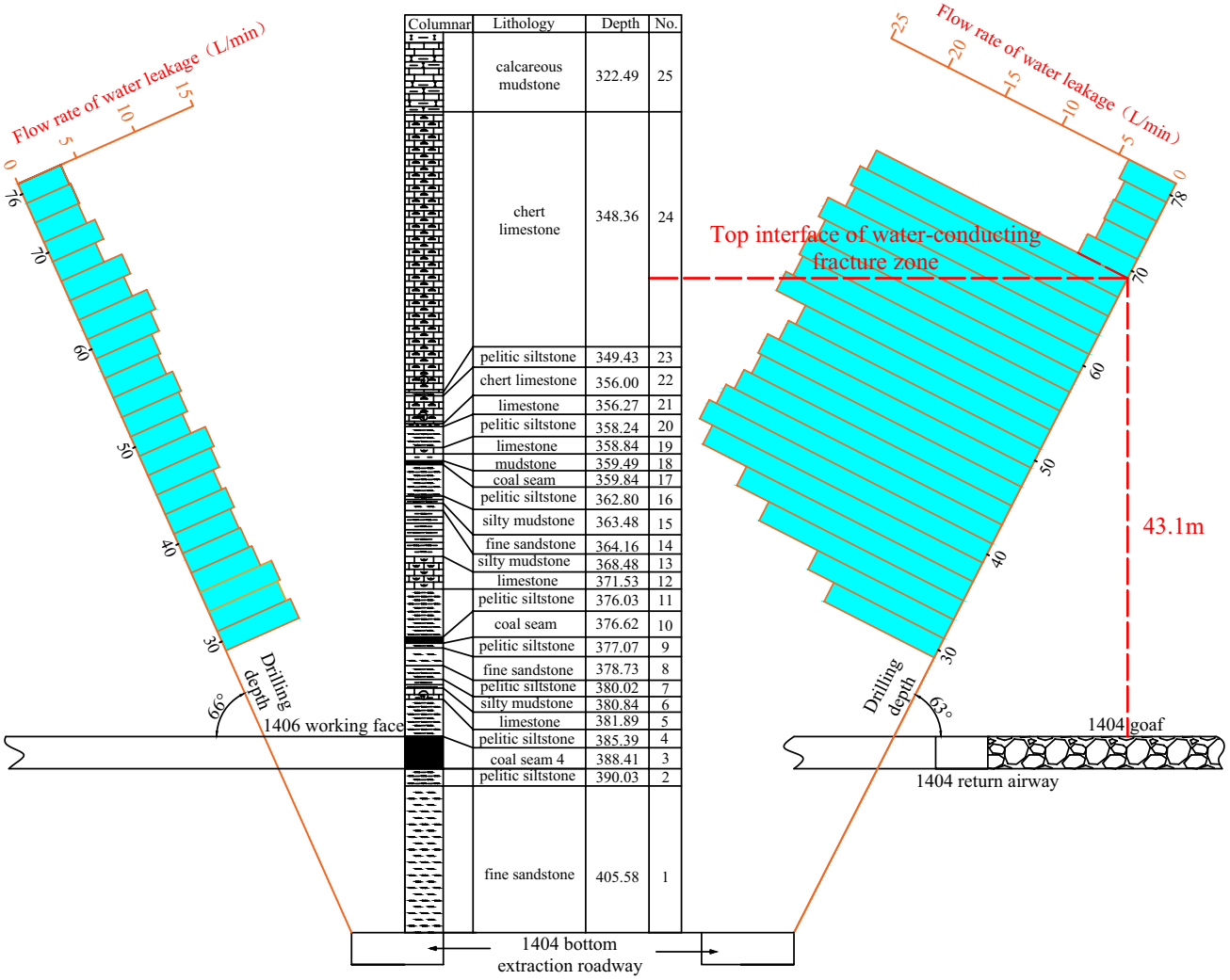

Fig. 2 Water leakage rate of comparative borehole and test Borehole

fractures threatened the safe mining of coal seam 4. The average water inflow of the mine from 2017 to 2020 was 81.8, 86.6, 90.0, and 116.5 m^3/h, respectively. The annual average rainfall increased gradually as the area of the mining face grew, causing increased damage to the overburden in general and the roof limestone aquifer in particular. The water inflow of the mine increased with the constant mining and as the annual rainfall increased.

Evolution of Water-Conducting Fractures in Roof Strata During Downward Mining

Field Measurement of the Height of the Water-Conducting Fracture Zone in the Mine Face

After one-month completion of mining in the 1404 working face, the double-end water-plugging leak detection was employed to obtain the development height of the water-conducting fracture zone in the mining face 1404 (Zhu et al. 2020). The borehole position was set in the bottom extraction roadway at the lower part of the no. 1404 mine face. A total of three boreholes were drilled: borehole 1 and 2 were test holes, and borehole 3 was the comparison borehole. The ZDY8000LPS crawler-type full hydraulic tunnel drill was used to construct and test the three exploration boreholes, as shown in Supplemental Fig. 3.

Figure 2 shows the water leakage of the different boreholes. The change rule of water leakage in the borehole section was analyzed, and then the development height of the water-conducting fracture zone of the overburden was determined. According to the water leakage results of borehole 3 (left side of Fig. 2), when the roof was not damaged, the average water leakage in the boreholes of the test section was 4.7 L/min, and the water leakage within the testing depth fluctuated, ranging from 3.1 to 5.1 L/min. Since borehole 1 collapsed during the test, the data of borehole 1 were ignored. According to the water leakage of borehole 2 (right side of Fig. 2), the water leakage was 3.5—5.0 L/min within the borehole depth of 68—78 m, which was consistent with the water leakage of the comparison borehole (borehole 3). It indicated that the rock strata in this section were undamaged. The water leakage increased within the borehole depth of 36—68 m, much more than in borehole 3, even reaching 19.2—22.3 L/min. This indicated that this section was the top interface of the water-conducting fracture zone. Therefore, the top interface of the roof water-conducting fracture zone determined by borehole 2 was located at the borehole depth of 68 m, where the vertical height from the coal seam roof was 43.1 m and the fracture mining ratio was 14.4.

Similarity Simulation of the Evolution of Water-Conducting Fractures in the Roof During Downward Mining

In this study, similar materials in the laboratory were employed to simulate the downward-inclined mining of coal seams 4 and 9, revealing how the water-conducting fractures in the overburden and the Yulongshan Member limestone aquifer evolved during downward mining.

Model Establishment

It was assumed during the establishment of the physical model of the mine that when water-conducting fractures developed to the bottom of the Yulongshan Member limestone, that a mine water inrush would be triggered. Hydraulic cylinder equivalent loading was used to simulate the unpaved rock layer in the model (Shi et al. 2019), using the geomechanical model support of Henan Polytechnic University. The support was 2.5 m in length, 0.2 m in width and 1.3 m in height, the geometric similarity ratio of the test model was 1:100, and the unit weight similarity ratio was 1:1.5. The height of the model and thickness of the coal seam were designed as 120 cm and 3.0 cm, and the dip angle was set as 3°. Fine dry river sand was used as aggregate in the model, borax was used as the retarder, and light calcium carbonate and gypsum as the cement. Mica flakes were used to layer the rock stratum. The 280 m thick overburden was not simulated in the model; instead, the hydraulic column on the test bench was used to simulate the equivalent loading (Sun et al. 2020). Table 1 shows the specific parameters of the similar simulation test.

A total of 69 displacement measuring points were set at 10 cm intervals in three displacement measuring lines (lines 1–3) at the back of the model. Line 1 was arranged at the top of the limestone of Changxing Formation, line 2 at the bottom of the limestone of Changxing Formation, and line 3 at the bottom of coal seam 4. Supplemental Fig. 4 shows the specific location of the displacement measuring lines.

Simulation Results and Analysis

Evolution of Water-Inrush Pathways in Downward Mining

Figure 3a and b shows the evolution characteristics of water-conducting fractures in the simulated coal seam 4

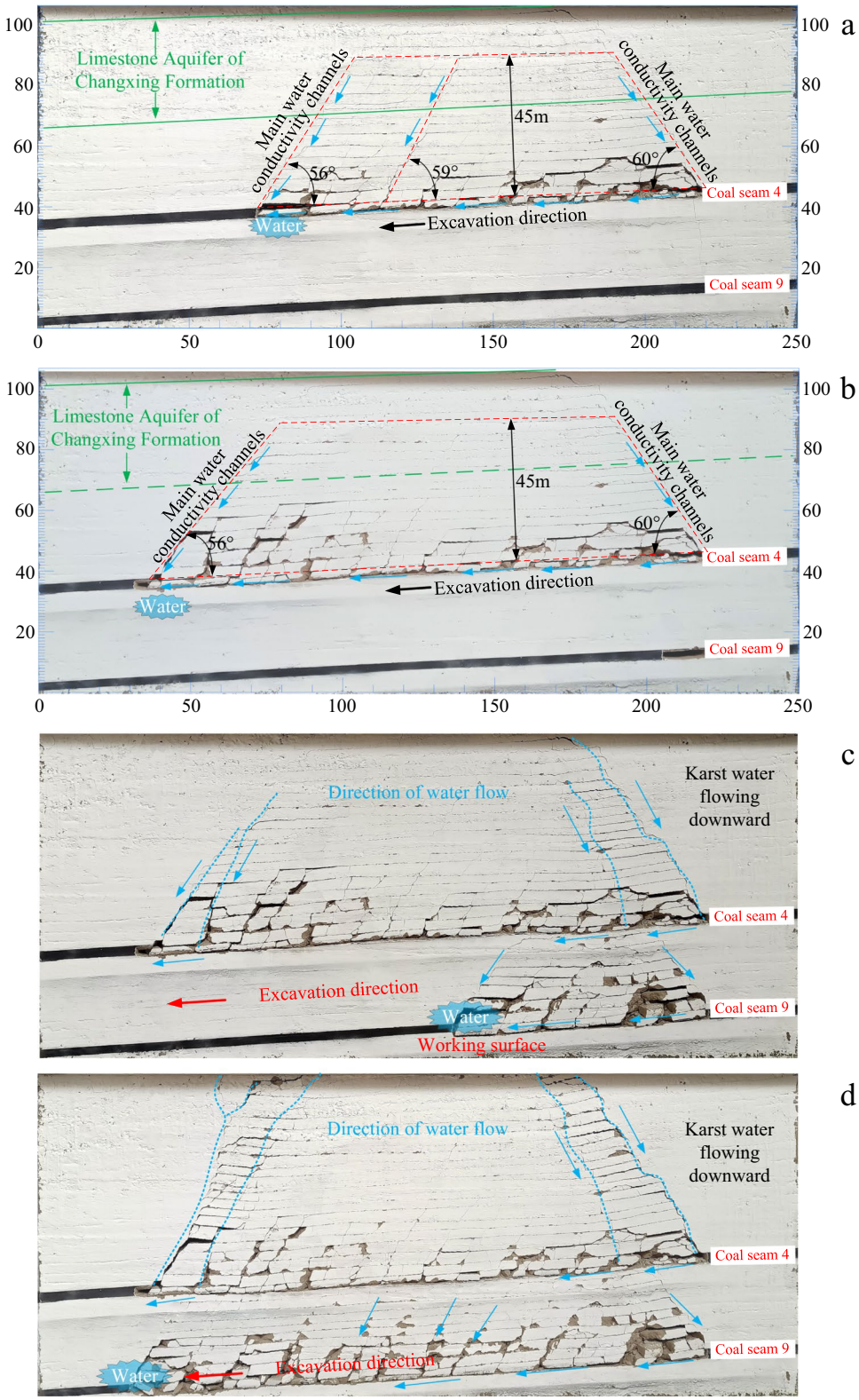

Fig. 3 Evolution Characteristics of Water-conducting Fractures in Roof of Coal Seam 4 and 9. **a** 150 m advancement in coal seam 4. **b** 190 m advancement in coal seam 4. **c** 85 m advancement in coal seam 9. **d** 190 m advancement in coal seam 9

roof strata under downward mining. After full extraction of the mining face, the fractures developed to the middle of the Changxing Formation limestone aquifer and open water-inrush pathways were generated behind the mining face and at the open-off cut. When the mining face had advanced to 150 m, three main water-inrush pathways formed behind the mining face. The angle of the main water-inrush pathways at the open-off cut was 60°, and

Table 1 Proportioning table of similar simulation test

No	Lithology	Compressive strength /MPa	Tensile strength /MPa	Strata thickness/m	Model thickness/ cm	Proportioning No	Sand/kg	Gypsum/kg	Calcium carbonate/ kg
1	Sand-mudstone	29.9	2.31	20.0	20.0	655	162.9	13.6	13.6
2	Limestone	51.40	5.70	35.0	35.0	437	266.0	20.0	46.6
3	Sand-mudstone	29.9	2.31	30.0	30.0	655	244.3	20.4	20.4
4	Coal seam 4	3.90	0.28	3.0	3.0	773	24.9	2.5	1.1
5	Sand-mudstone	29.9	2.31	29.0	29.0	655	236.1	19.7	19.7
6	Coal seam 9	3.90	0.28	3.0	3.0	773	24.9	2.5	1.1

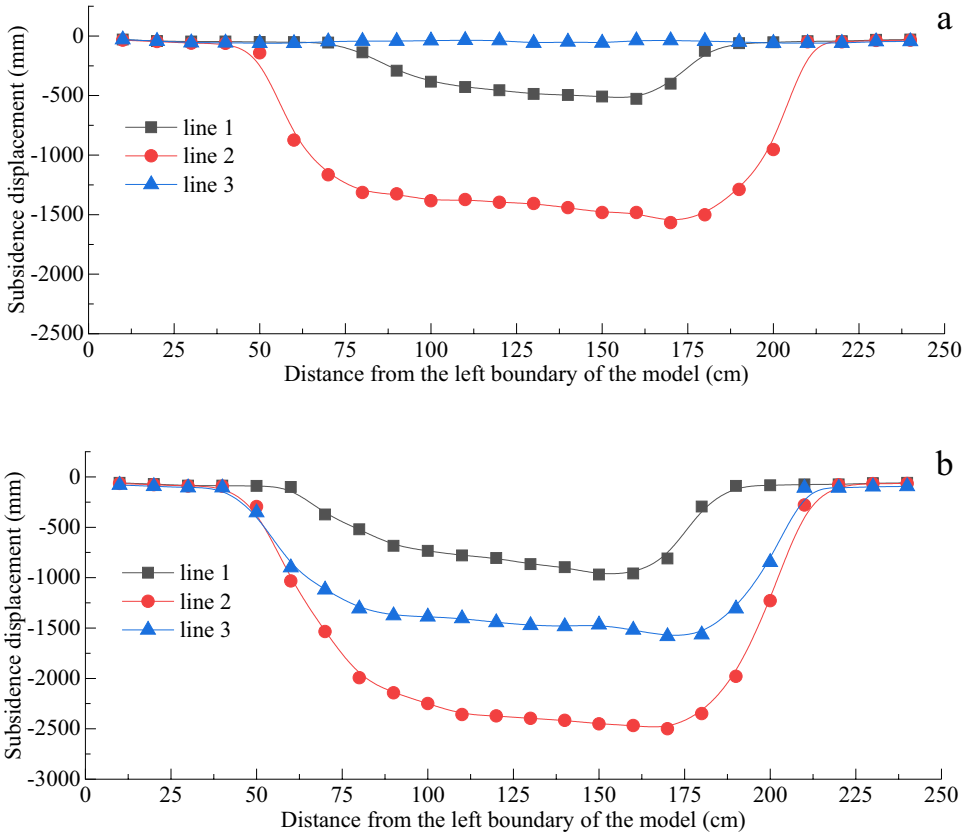

Fig. 4 Roof Subsidence Displacement Curve. **a** excavation of coal seam 4. **b** excavation of coal seam 9

the angles of the two main water-inrush pathways behind the mining face were 56° and 59°, respectively. The maximum development height of the water-conducting fracture was 45 m. When the mining face had advanced to 190 m, periodic fractures occurred again in the roof, and a new water-inrush pathway formed behind the mining face. However, these fractures no longer developed upward, and the fracture mining ratio was 15.0. The water-inrush pathway far from the mining face gradually closed, and the water-conducting capacity gradually weakened. Nevertheless, there were always two large water-inrush pathways behind the mine face through which water in the aquifer could continuously flow. As a result, the mine face will always be affected by roof water inflow.

Figures 3c and d shows the evolution characteristics of water-conducting fractures in the roof of coal seam 9 under downward mining. When the simulated mine face had advanced to 85 m, periodic fractures occurred in the roof and the fractures developed to the goaf of coal seam 4. With continuous advancement of coal seam 9, new longitudinal fractures continuously formed in the roof, which served as the downward water-inrush pathway of the coal

seam 4 goaf. Roof karst water constantly affected mine production in coal seam 9.

Movement and Deformation Characteristics of Overburden in Downward Mining

Figure 4 shows the movement and deformation characteristics of the overburden of coal seams 4 and 9 under downward mining. After the downward mining of coal seam 4, the lower and upper parts of the Changxing Formation limestone aquifer had moved and deformed to varying degrees, while the displacement of line 3 at the bottom of coal seam 4 had changed little (see Fig. 4a). Line 1 is located at the top of the Changxing Formation limestone aquifer, and the rock strata at the position of line 1 only bend and sink, which is less affected by mining. Line 2 is located at the bottom of the Changxing Formation limestone. Under the influence of mining, the rock strata at line 2 were broken and collapsed, with large displacement and deformation. The displacement of rock strata near the open-off cut was obviously larger than that near the stop-mining line. The main reason is that the rock stratum at the side of the cut hole slip towards the stop-mining line under the influence of gravity, which further aggravates the subsidence of rock strata on the right side of the model. After the downward mining of coal seam 9, the floor of coal seam 4 was broken and subsided, the displacement of the rock strata near line 3 changed greatly, and the rock strata near lines 1 and 2 were further moved and deformed due to the mining of coal seam 4 (Fig. 4b).

Water Inrush Control Technology of a Karst Roof

Basic Principle of Roof Water Inrush Control During Upward Mining

Considering that the two coal seams were threatened by roof water inrush during downward mining, the spatio-temporal evolution law of the water-conducting fractures in downward mining of close coal seams were referred to, and it was decided to assess roof water inrush during upward mining (with coal seam 9 being mined first, followed by coal seam 4). Since coal seam 9 was far from the roof aquifer, the mining face there should not be threatened by roof karst water during extraction. Then, during the extraction of coal seam 4, the water-conducting fractures produced by the extraction of coal seam 9 should serve as a water-inrush pathway; the water could flow from the roof behind the mining face into the goaf of coal seam 9, avoiding the adverse impact on the mining of coal seam 4.

Theoretical Analysis of the Feasibility of Upward Mining

The ratio test and "three zones" discrimination method were used to explore the feasibility of upward mining (Liu et al. 2022).

The ratio test: In the ratio test, the mining influence coefficient K is taken as the standard. Specifically, when a single coal seam is mined at its lowest part, the mining of the upper coal seam can only be carried out if the mining influence coefficient $K>5.5$ is met (Shi et al. 2020), where the mining influence coefficient K is:

$$K = \frac{H}{M} \tag{1}$$

where H is the distance (in m) between the lower and upper coal seams and M is the mining thickness of the lower coal seam. According to the geological conditions of the Xintian Coal Mine, coal seam 4 is 29.0 m above coal seam 9, and the mining thickness of coal seam 9 is 3.0 m. The mining influence coefficient of coal seam 9 on the upper coal seam 4 was thus calculated to be 9.7, indicating that upward mining is feasible.

The "Three zones" discrimination method: The roof strata of coal seams 4 and 9 are mostly sandstone with moderate hardness. The theoretical development height of the caving zone and the water-conducting fracture zone can be obtained by the following equations.

$$\text{Caving zone}: H_L = \frac{100\Sigma M}{1.6\Sigma M + 3.6} \pm 5.6 \tag{2}$$

$$\text{Fracture zone}: H_L = 20\sqrt{\Sigma M} + 10 \tag{3}$$

$$\text{Caving zone}: H_m = \frac{100\Sigma M}{4.7\Sigma M + 19} \pm 2.2 \tag{4}$$

The mining height of coal seam 9 is ≈3.0 m. The height of the mining-induced caving zone is 6.7—11.3 m, and the height of the fracture zone is 30.1—44.6 m. Coal seam 4 is 29.0 m above coal seam 9, which is in the upper part of the water-conducting fracture zone, and coal seam 4 is less affected by mining. Therefore, this approach also indicates that upward mining should be feasible.

Similar Simulation Study on Upward Mining Feasibility

Overburden Fracture Characteristics of Upward Mining

To further assess the feasibility of upward mining, a physical similarity model was built, using the same physical and mechanical parameters, model size, and ratio number of rock strata as the downward mining model. However, the excavation sequence was changed. Specifically, coal seam 9 was mined first, followed by coal seam 4, and the fracture evolution for upward mining was mastered.

As the mining face of coal seam 9 advanced to 85 m, the overburden fractured to the floor of coal seam 4, and layer separation occurred in the floor. As the mining face advanced to 105 m, the overburden fracture continued to develop upward, extending the fracture development height to 27.0 m. With the continuous advance of the mining face,

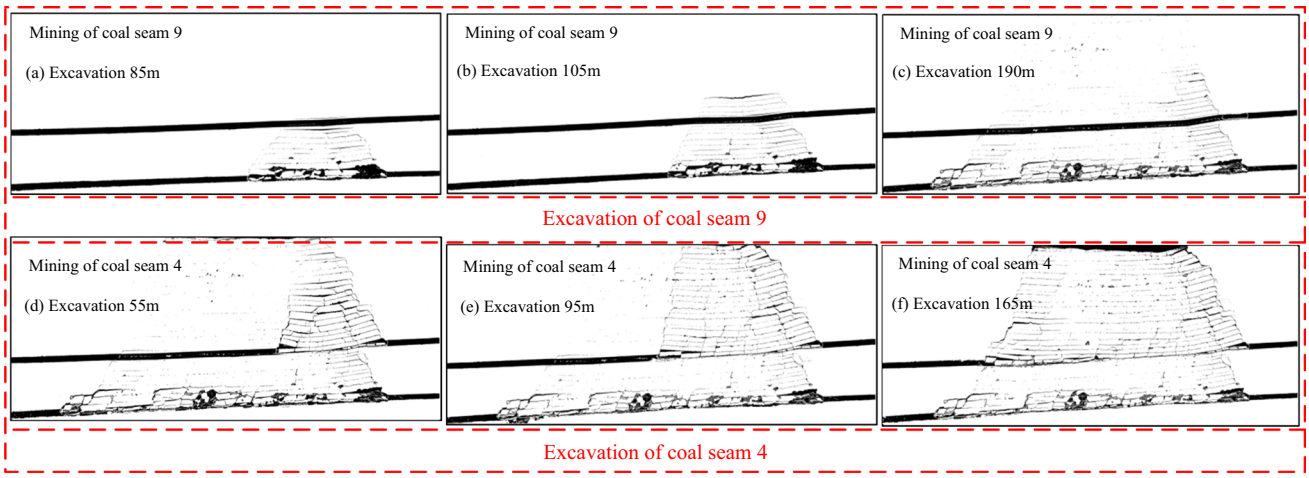

Fig. 5 Overburden Fracture Characteristics of coal seams 4 and 9 in Downward Mining

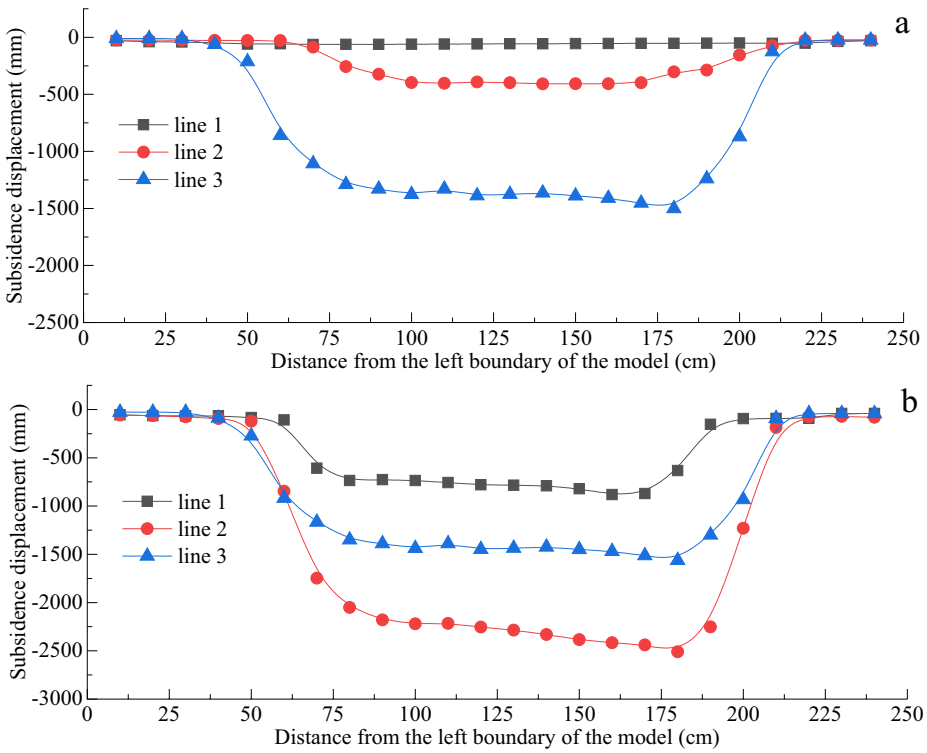

Fig. 6 Variation Curve of Roof Subsidence Displacement during Upward Mining. **a** the excavation of coal seam 9. **b** the excavation of coal seam 4

fractures periodically occurred in the roof, but the cracks no longer developed upward. At that time, the maximum crack development height was 45.0 m, which is located at the side of the open-off cut. As the mining face of coal seam 4 advanced to 55 m, the periodic fracturing of the roof occurred, and the fractures on the side of the open-off cut developed to the top of the model, which was connected with the upper part of the Yulongshan limestone aquifer. With constant excavation of coal seam 4, the periodic fracturing occurred in the roof almost constantly, and many water-inrush pathways connecting with the upper aquifer were generated. Meanwhile, the goaf behind the mining face continued to sink and compact, the cracks gradually closed, and there was always a through water-inrush pathway at the sides of the open-off cut and the mining face.

Figure 5 shows the movement and deformation characteristics of overburden of coal seams 4 and 9 during upward mining. The subsidence on the right side of the model was greater than on the left. After downward mining of coal seam 9, the floor of coal seam 4 was damaged and deformed, and the maximum subsidence displacement of line 3 was -1.5 m (Fig. 6a). The upper part of the Changxing Formation limestone was less affected by mining, and the subsidence displacement of line 1 was small. The lower part of the Changxing Formation limestone is subject to bending deformation under the influence of mining, and the maximum subsidence value was -0.4 m. After coal seam 4 was subjected to downward mining, the Changxing Formation limestone was fractured and deformed. The maximum subsidence value of line 1 was −0.9 m, and that of line 2 was −2.5 m. Due to the mining of coal seam 4, the rock mass between coal seams 4 and 9 were further compacted, and the rock strata of line 3 were further deformed and subsided (Fig. 6b).

Figure 6 will be inserted near here during the final printing process.

Fracture Development During Upward Mining

Figure 7a shows fracture development characteristics after the upward mining of coal seam 9. The mining-induced fracture of coal seam 9 penetrated coal seam 4 and developed to the bottom of the Changxing limestone formation. Because the dip angle affects the movement of rock strata to the lower left, the fractures are relatively developed at the open-off cut. Figure 8 shows the variation curve of the overburden fracture height of coal seam 9 during upward mining. When coal seam 9 advanced to 145 m, the overburden fracture height reached its maximum (i.e. 47.0 m), and the fracture mining ratio was 15.7. At that time, the maximum development height of the water-conducting fracture was located at the Changxing Formation limestone floor.

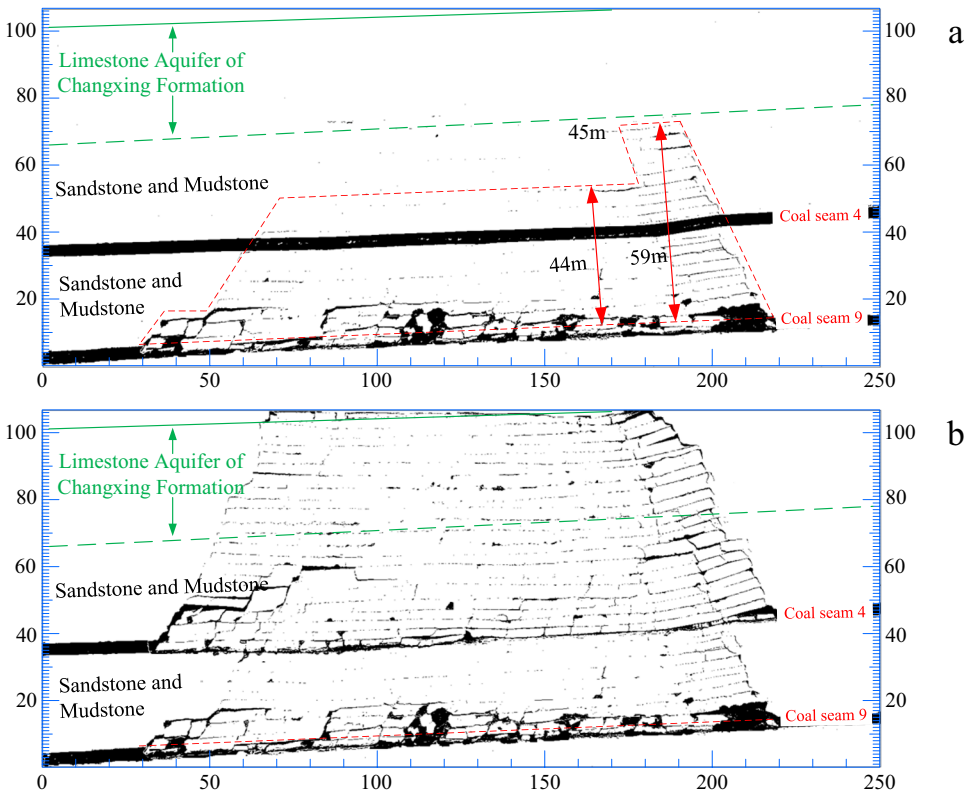

Fig. 7 Development Characteristics of Roof fracture in Upward Mining. **a** fracture field of coal seam 9 during upward mining. **b** fracture field of coal seam 9 during upward mining

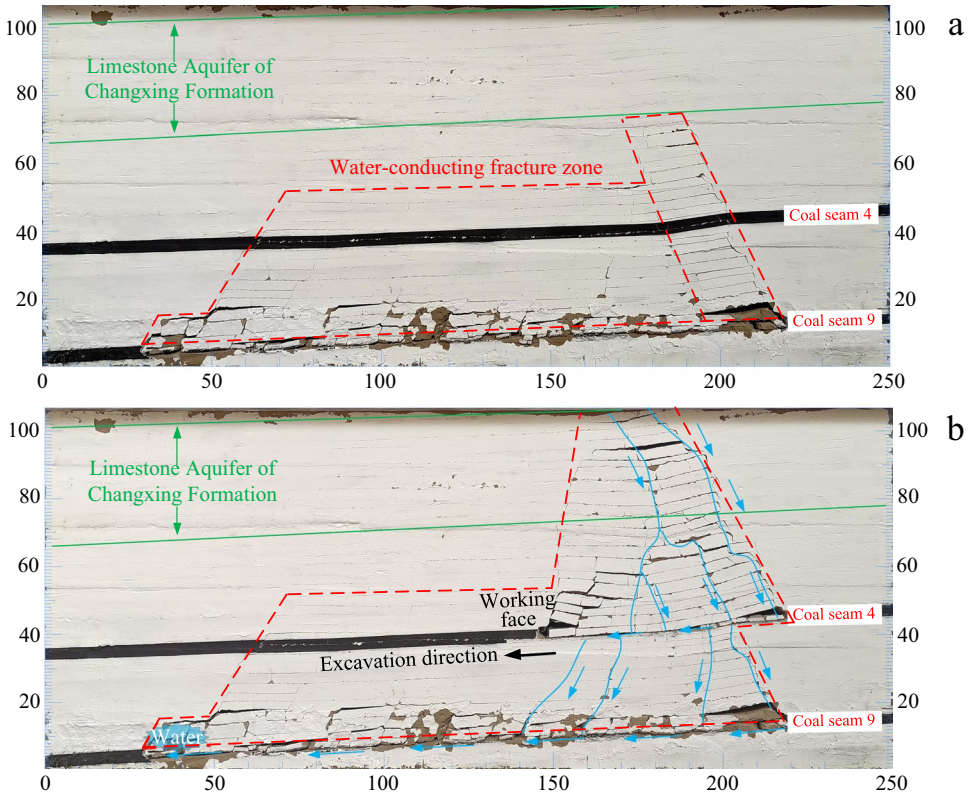

Fig. 8 Development Characteristics of Water inrush Pathway in Roof during Upward Mining. **a** 190 m advancement in coal seam 9. **b** 75 m advancement in coal seam 4

Figure 7b shows a sketch map of the fracture field formed after the upward mining of coal seam 4. The roof subsidence increased with the extraction of coal seam 4, and the roof fracture of coal seam 4 completely penetrated the entire model. The mining of coal seam 4 significantly affected the stability of the coal seam 9 goaf, and the upper rock of the goaf of coal seam 9 was further compacted, but there were still several water-conducting fractures running through coal seams 4 and 9.

Comparison and Analysis of Water-Inrush Pathways During Upward And Downward Mining

The development of water-conducting fractures were compared and analyzed under different mining sequences. We concluded that upward mining is superior to downward mining under these conditions. As shown in Fig. 3a, when coal seam 4 advanced 150 m in downward mining, roof water can flow into the goaf through the original and mining-induced fractures, and the roof water flowed to the mining face until the mining of coal seam 4 was completed. During the extraction of coal seam 9, the roof water entered the goaf of coal seam 9 through water-conducting fractures from the goaf of coal seam 4, as shown in Fig. 8a. Due to the inclined mining, the karst water will flow to the mining face. Therefore, the threat of roof water cannot be removed from the downward mining of the two layers of coal seams.

As shown in Fig. 8a, when coal seam 9 advanced to 190 m by downward mining, mining-induced water-conducting fractures were only generated above the open-off cut on the right side of the model and developed to the limestone floor of the Changxing Formation. As the mining face constantly advanced, the height of the water-conducting fractures did not extend to the bottom of the limestone of the Changxing Formation. This indicates that the whole mining face will not be fully connected with the limestone aquifer of Changxing Formation, nor the strong aquifer of the Yulongshan Member in the upper part. Therefore, the mining of coal seam 9 is free from the roof karst water hazard. As shown in Fig. 8b, when coal seam 4 was mined for 75 m, the mining-induced fracture in the roof developed to the Changxing Formation limestone aquifer, allowing the karst water in this aquifer to flow into the goaf of coal seam 4 through fractures. However, the karst water enters the goaf of coal seam 9 through the floor fractures during the mining of coal seam 4, avoiding the threat of roof karst water during the

Table 2 Monitoring results of underground water samples

Test items	PH	Chroma	Turbidity	Olfaction	Chloride (mg/L)	Fluoride (mg/L)	Ammonia nitrogen (mg/L)	Iron (mg/L)	Manganese (mg/L)	Total dissolved solids (mg/L)
Standard	6–9	≤ 30	≤5	No pungent taste	≤250	≤ 1.0	≤5	≤0.3	≤0.1	≤1000
Sample 1	8.8	10	7.0	Weak	6.67	0.48	1.41	0.03	0.01	436.9
Sample 2	8.4	0	5.0	No	3.0	0.55	1.59	0.03	0.01	337.0

extraction of coal seam 4. Therefore, upward mining can effectively control the problem of karst water in the coal seam roof.

The Technology and Process of Water Extraction from the Goaf of the Lower Group Coal

Based on the feasibility analysis of upward mining, we proposed the co-mining of coal and water, where the water would be extracted from the goaf of the lower coal group. As the karst water in Yulongshan Member enters the water storage space of coal seam 9 through the mining-induced fractures, which can be directly used for mine production after natural precipitation and simple purification. Although the annual rainfall is large, the mine is located in a rocky desert area with a thin topsoil layer, rare surface vegetation, and large evaporative capacity, leading to scarce surface water resources. To ensure normal mine production, attention should be paid to the recycling of mine water resources.

Water samples were collected in the Xintian Mine goaf and analyzed. Table 2 shows that the quality of the karst water is good. The average pH value of the wastewater in the goaf is 8.6, which is weakly alkaline. The content of fluoride, sulfate, and nitrate is less than the production water standard, and all indicators attained the latest standard of *Code for design of the fire-protecting, sprinkling system in underground coal mine* (GB50383-2016) and *The reuse of urban recycling water—Water quality standard for urban miscellaneous water consumption* (GB/T18920-2020). Alternatively, after simple treatment by surface water treatment plants, the underground water can be used for domestic water (Fig. 9).

The surrounding rock and coal seam in the Xintian mine contain very few harmful substances. After simple treatment, the mine water can be used for underground production, green environmental protection, mining area drinking water, gas power plant water, industrial production, and construction water. In addition, the remaining mine water can be supplied to the surrounding villages for domestic use and farmland irrigation. Figure 10 shows the process of utilizing the mine water resources.

Conclusion

1. The coal mining in the karst area of western Guizhou is threatened by karst water in the roof, and the mine water inflow is positively related to atmospheric precipitation. As mining progresses, the damaged area of

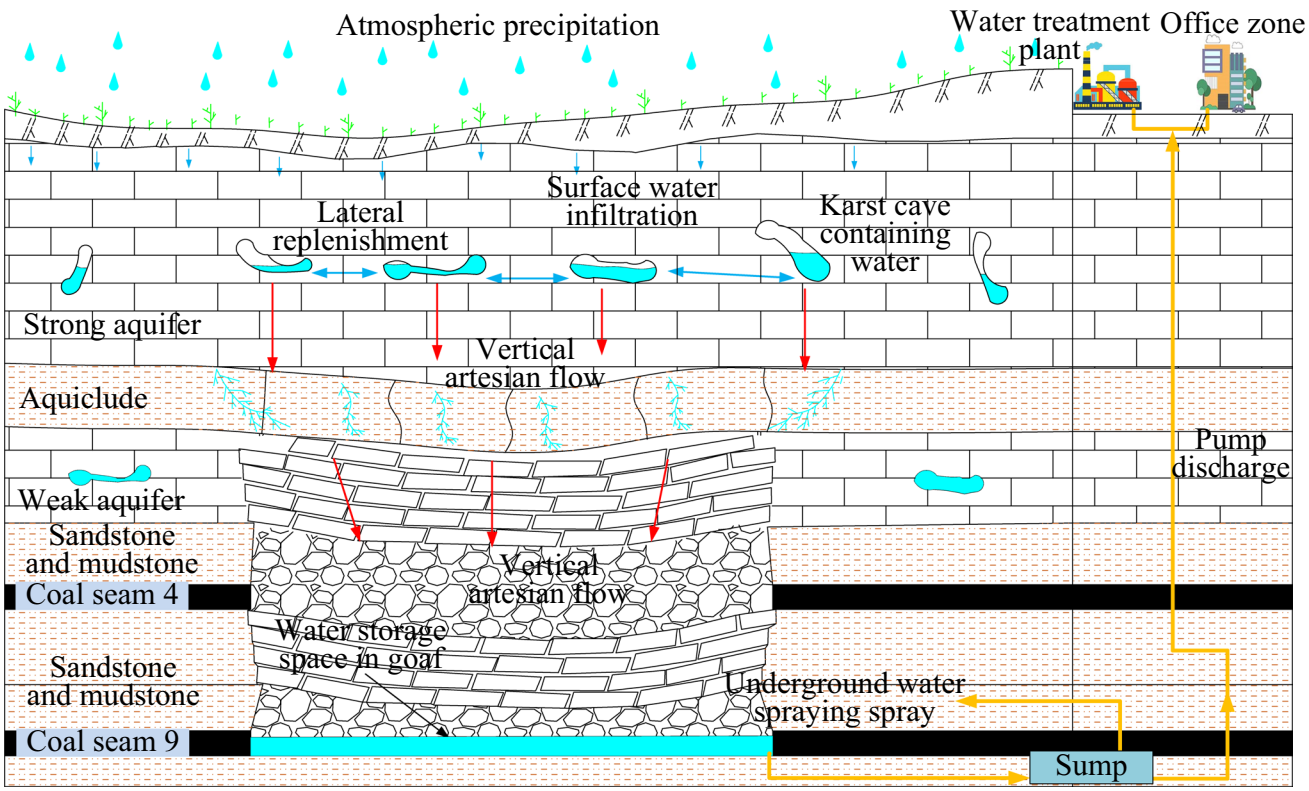

Fig. 9 Schematic diagram of coal-water co-mining technology

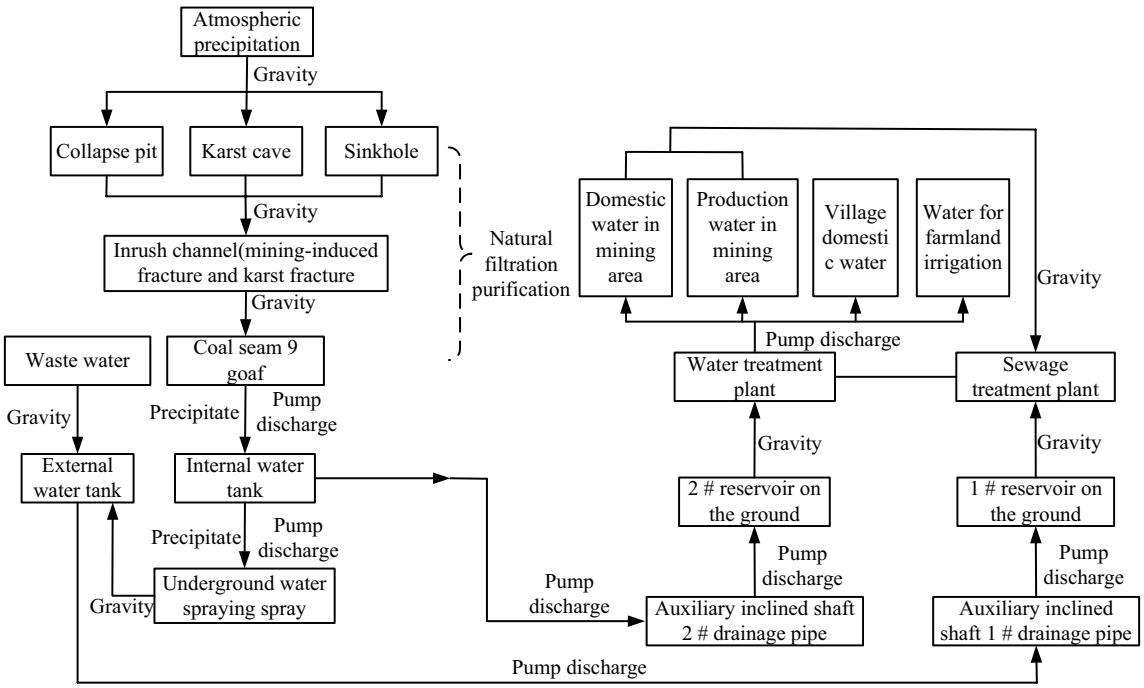

Fig. 10 Mine water resources utilization process

the roof limestone aquifer is becoming larger and larger. It is estimated that the mine water inflow will increase with continued mining, which threatens the safe mining of coal seam 4.

2. By using double-end water-plugging detection, we determined that the maximum development height of the water-conducting fracture zone above coal seam 4 is 43.1 m, the fracture mining ratio is 14.4, and the fracture has developed to the middle of the Changxing Formation limestone. At the same time, the physical similarity simulation we employed revealed the evolution characteristics of water-conducting fractures and the evolution of the water-inrush pathway that will accompany the mining of coal seams 4 and 9. The results show that the mining of coal seams 4 and 9 will be threatened by roof water during downward-inclined mining.
3. Two mining methods, upward and downward mining, were investigated based on the height of the water-conducting fractures in the overlying formations. The upward mining method is recommended to avoid the threat of karst water to the underground mining panels from the overlying aquifer. Both the ratio test and "three zones" discrimination methods indicate that upward mining is feasible.
4. Based on our research results, the co-mining of the natural karst water and the coal is proposed. Using inclined fully mechanized mining and upward mining should avoid the threat of karst roof water to the mining face. After mining, the goaf in the lower coal group will be used for water resource storage and utilization. This technology will improve both mining production and water protection in the mining area, and also provides new insight into the potential of coal-water co-mining in China's southwest mining area.
5. Since it was not possible to field test the proposed upward mining method, simulation experiments with appropriate scaling and boundary effects were used to research the anticipated height of the water-conducting fractures. Future research will involve selecting an appropriate upward mining test site, and testing the approach using microseismic monitoring, electrical monitoring, and other methods.

Supplementary Information The online version contains supplementary material available at https://doi.org/10.1007/s10230-023-00953-3.

Acknowledgements This research was funded by National Natural Science Foundation of China (52174073, 52004082); Henan Natural Science Foundation of China (222300420007); Henan University Science and Technology Innovation Team Support Program of China (23IRTSTHN005).

References

Chen Y, Zhu SY (2020) Determination of caved and water-conducting fractured zones of "two soft and one hard" unstable coal seam. Acta Geod Geophys 55:451–475. https://doi.org/10.1007/s40328-020-00300-w

Chen LW, Ou QH, Peng ZH, Wang YX, Chen YF, Tian Y (2022) Numerical simulation of abnormal roof water-inrush mechanism in mining under unconsolidated aquifer based on overburden dynamic damage. Eng Fail Anal. https://doi.org/10.1016/j.engfailanal.2021.106005

Chen YM, Zhang Y, Xia F, Xing Z, Wang LC (2022) Impacts of underground reservoir site selection and water storage on the groundwater flow system in a mining area-a case study of the Daliuta Mine. Water (Basel). https://doi.org/10.3390/w14203282

Cheng GW, Yang TH, Liu HY, Wei LK, Zhao Y, Liu YL, Qian JW (2020) Characteristics of stratum movement induced by downward longwall mining activities in middle-distance multi-seam. Int J Rock Mech Min Sci 1997:136. https://doi.org/10.1016/j.ijrmms.2020.104517

Dong SN, Xu B, Yin SX, Han Y, Zhang XD, Dai ZX (2019) Water resources utilization and protection in the coal mining area of northern China. Sci Rep. https://doi.org/10.1038/s41598-018-38148-4

Dong SN, Wang H, Guo XM, Zhou ZF (2021) Characteristics of water hazards in China's coal mines: a review. Mine Water Environ 40:325–333. https://doi.org/10.1007/s10230-021-00770-6

Feng J, Wang SJ, Hou EK, Ding X, Duan HJ (2021) Determining the height of water-flowing fractured zone in bedrock-soil layer in a Jurassic coalfield in northern Shaanxi China. Adv Civ Eng. https://doi.org/10.1155/2021/9718802

Gui HR, Tong SJ, Qiu WZ, Lin ML (2018) Research on preventive technologies for bed-separation water hazard in China coal mines. Appl Water Sci. https://doi.org/10.1007/s13201-018-0667-0

Ji YD, Cao HD, Zhao BF (2021) Mechanism and control of water inrush from separated roof layers in the Jurassic Coalfields. Mine Water Environ 40:357–365. https://doi.org/10.1007/s10230-021-00755-5

Jiang CF, Gao XB, Hou BJ, Zhang ST, Zhang JY, Li CC, Wang WZ (2020) Occurrence and environmental impact of coal mine goaf water in karst areas in China. J Clean Prod. https://doi.org/10.1016/j.jclepro.2020.123813

Jiang N, Wang CX, Pan HY, Yin DW, Ma JB (2020b) Modeling study on the influence of the strip filling mining sequence on mining-induced failure. Energy Sci Eng 8:2239–2255. https://doi.org/10.1002/ese3.660

Ju F, Xiao M, Guo S, Li BY (2018) Geological characteristics of the main aquifer coal seam in the Ordos Basin coalfield, China. Arab J Geosci. https://doi.org/10.1007/s12517-018-4008-2

Kumari W, Ranjith PG (2019) Sustainable development of enhanced geothermal systems based on geotechnical research - a review. Earth Sci Rev. https://doi.org/10.1016/j.earscirev.2019.102955

Li CT, Wu SY, Zheng CS, Sun XY, Jiang XQ (2022a) Study on temporal and spatial evolution characteristics of overburden deformation and gas emission during the longwall working face initial mining phase. J Geophys Eng 19:534–549. https://doi.org/10.1093/jge/gxac031

Li Q, Wu GY, Kong DZ, Han S, Ma ZQ (2022) Study on mechanism of end face roof leaks based on stope roof structure movement under repeated mining. Eng Fail Anal. https://doi.org/10.1016/j.engfailanal.2022.106162

Li YY, Zhang S, Yang YM, Chen HR, Li ZK, Ma Q (2022c) Study on the water bursting law and spatial distribution of fractures of mining overlying strata in weakly cemented strata in West China. Geomech Eng 28:613–624. https://doi.org/10.12989/gae.2022.28.6.613

Liu SL, Li WP, Wang QQ, Pei YB (2018) Investigation on mining-induced fractured zone height developed in different layers above Jurassic coal seam in western China. Arab J Geosci. https://doi.org/10.1007/s12517-018-3383-z

Liu YB, Cheng JL, Jiao JJ, Meng XX (2022) Feasibility study on multi-seam upward mining of multi-layer soft-hard alternate complex roof. Environ Earth Sci. https://doi.org/10.1007/s12665-022-10537-z

Long TW, Hou EK, Xie XS, Fan ZG, Tan EM (2022) Study on the damage characteristics of overburden of mining roof in deeply buried coal seam. Sci Rep. https://doi.org/10.1038/s41598-022-15220-8

Menendez J, Ordonez A, Fernandez-Oro JM, Loredo J, Diaz-Aguado MB (2020) Feasibility analysis of using mine water from abandoned coal mines in Spain for heating and cooling of buildings. Renew Energy 146:1166–1176. https://doi.org/10.1016/j.renene.2019.07.054

Qiu Q, Zheng LL, Lan H, Zhang W, He HY, Zhao C, Tian YW, Liu H, Li RP (2022) Water inrush mechanism of roof induced by the fault weakening effect in coal mining. Math Probl Eng. https://doi.org/10.1155/2022/5737738

Shi LQ, Xu DJ, Wang Y, Qiu M, Hao J (2019) A novel conceptual model of fracture evolution patterns in the overlying strata during horizontal coal seam mining. Arab J Geosci. https://doi.org/10.1007/s12517-019-4486-x

Shi LQ, Qu XY, Yu XG, Li Y, Pei FH, Qiu M, Gao WF (2020) Theory and practice on the division of the "water pressure-free zone" in a mining coal seam floor. Arab J Geosci. https://doi.org/10.1007/s12517-020-06067-2

Song HQ, Xu JJ, Fang J, Cao ZG, Yang LZ, Li TX (2020) Potential for mine water disposal in coal seam goaf: Investigation of storage coefficients in the Shendong mining area. J Clean Prod. https://doi.org/10.1016/j.jclepro.2019.118646

Sun Q, Meng GH, Sun K, Zhang JX (2020) Physical simulation experiment on prevention and control of water inrush disaster by backfilling mining under aquifer. Environ Earth Sci. https://doi.org/10.1007/s12665-020-09174-1

Sun BY, Zhang PS, Wu RX, Fu MR, Ou YC (2021) Research on the overburden deformation and migration law in deep and extra-thick coal seam mining. J Appl Geophy. https://doi.org/10.1016/j.jappgeo.2021.104337

Suo J, Qin QR, Wang WQ, Li ZH, Huang CH, Xu YL, Chen ZG (2022) Disastrous mechanism of water burst by karst roof channel in rocky desertification mining area in southwest China. Geofluids. https://doi.org/10.1155/2022/7332182

Wen P, Guo WB, Tan Y, Bai EH, Ma ZB, Wu DT, Yang WQ (2022) Paste backfilling longwall mining technology for thick coal seam extraction under buildings and above confined aquifers: a case study. Minerals (Basel). https://doi.org/10.3390/min12040470

Xiao Y, Hou B, Liu X, Cao BW, Muhadasi Y, Ling CQ, Xie L (2020) Fine calculation method for fracture morphology based on microseismic events and its application. Energy Sci Eng. https://doi.org/10.1002/ese3.523

Xu B, Yue ZW, Li YL, Wang SS, Li J, Lu B (2022) Research on the control of overburden deformation by filling ratio of cementing filling method with continuous mining and continuous backfilling. Environ Sci Pollut Res Int. https://doi.org/10.1007/s11356-022-24038-w

Yao WL, Yang Z, Guo XY (2019) Fracture development in large-scale overburden strata induced by longwall mining. Energy Sources Part A-Recovery Util Environ Eff 41:269–279. https://doi.org/10.1080/15567036.2018.1516008

Zha H, Liu WQ, Liu QH (2020) Physical simulation of the water-conducting fracture zone of weak roofs in shallow seam mining based on a self-designed hydromechanical coupling experiment system. Geofluids. https://doi.org/10.1155/2020/2586349

Zhang PF, Lu SF, Li JQ (2019) Characterization of pore size distributions of shale oil reservoirs: a case study from Dongying Sag, Bohai Bay basin, China. Mar Pet Geol 100:297–308. https://doi.org/10.1016/j.marpetgeo.2018.11.024

Zhang SY, Wang H, He XW, Guo SQ, Xia Y, Zhou YX, Liu K, Yang SP (2020) Research progress, problems and prospects of mine water treatment technology and resource utilization in China. Crit Rev Environ Sci Technol 50:331–383. https://doi.org/10.1080/10643389.2019.1629798

Zhang C, Wang FT, Bai QS (2021) Underground space utilization of coalmines in China: a review of underground water reservoir construction. Tunn Undergr Space Technol. https://doi.org/10.1016/j.tust.2020.103657

Zhang M, Chen LW, Yao DX, Hou XW, Zhang J, Qin H, Ren XX, Zheng X (2022) Hydrogeochemical processes and inverse modeling for a multilayer aquifer system in the Yuaner Coal Mine, Huaibei Coalfield, China. Mine Water Environ 41:775–789. https://doi.org/10.1007/s10230-022-00851-0

Zhao GZ, Zhang BS, Zhang LH, Liu C, Wang S (2021) Roof fracture characteristics and strata behavior law of super large mining working faces. Geofluids. https://doi.org/10.1155/2021/8530009

Zhu TG, Li WP, Wang QQ, Hu YB, Fan KF, Du JF (2020) Study on the height of the mining-induced water-conducting fracture zone under the Q(2l) loess cover of the Jurassic coal seam in northern Shaanxi, China. Mine Water Environ 39:57–67. https://doi.org/10.1007/s10230-020-00656-z

Zhu J, Jin S, Yang Y, Zhang TY (2022) Geothermal resource exploration in magmatic rock areas using a comprehensive geophysical method. Geofluids. https://doi.org/10.1155/2022/5929324

Zhu L, Song TQ, Gu WZ, Xu K, Liu ZC, Qiu FQ, Zhang XF (2022) Study on layered-backfill-based water protection technology of thick coal seam in the ecologically fragile mining area in western China. Geofluids. https://doi.org/10.1155/2022/3505176